Proc. Natl. Acad. Sci. USA
Vol. 86, pp. 6802–6806, September 1989
Neurobiology

Transient low-threshold Ca^{2+} current triggers burst firing through an afterdepolarizing potential in an adult mammalian neuron

(ion currents/dorsal root ganglia/epilepsy/repetitive firing)

GEOFFREY WHITE*, DAVID M. LOVINGER, AND FORREST F. WEIGHT

Section of Electrophysiology, Laboratory of Physiologic and Pharmacologic Studies, National Institute on Alcohol Abuse and Alcoholism, Rockville, MD 20852

Communicated by Eric R. Kandel, June 12, 1989

ABSTRACT **In a variety of mammalian neurons, a brief depolarization generates an afterdepolarizing potential that triggers the firing of a short series or burst of action potentials. Although such burst firing is thought to contribute to the processing of neural information, the ionic currents that underlie this phenomenon have not been established. In whole-cell patch-clamp experiments on dorsal root ganglion neurons, we have found that the current that underlies this type of burst firing is a transient low-threshold (T-type) Ca^{2+} current. The data suggest that the T-type Ca^{2+} current may play an important role in the processing of information in the nervous system by virtue of its ability to elicit burst firing in neurons.**

In the nervous system, information is encoded by neurons as the number and/or frequency of action potentials. In several types of mammalian neurons, a brief depolarizing event can elicit a burst of action potentials (1–4). Such burst-firing activity and its regulation are thought to play an important role in neuronal information processing (5–7) and may also contribute to epileptiform activity (8, 9). The burst-firing phenomenon is the result of the intrinsic electrical properties of certain neurons (7); however, the membrane ion currents that underlie this phenomenon have not been determined in voltage-clamp experiments on adult mammalian neurons. We have studied the ionic currents involved in the generation of burst firing in a subpopulation of adult rat dorsal root ganglion (DRG) neurons by using the whole-cell patch-clamp technique and report here that a transient low-threshold (T-type) Ca^{2+} current generates an afterdepolarizing potential (ADPP) that triggers burst firing in these neurons.

METHODS

Neuronal somata were isolated using enzymatic and mechanical means. Adult male Sprague–Dawley rats (100–400 g) were sacrificed by decapitation; DRGs were dissected from the upper lumbar to midthoracic regions of the vertebral column and minced 2 or 3 times with iridectomy scissors. DRGs were then placed in a flask containing 5 ml of Dulbecco's modified Eagle's medium in which trypsin (10,000 units/ml, Sigma type III), collagenase (1 mg/ml, Sigma type 1A), and DNase (0.1 mg/ml, Sigma type III) had been dissolved. Cells were incubated for 50–60 min at 35°C, and then soybean trypsin inhibitor (Sigma type IIs) was added in a quantity sufficient to neutralize twice the amount of added trypsin. Neurons were then distributed into uncoated Petri dishes and used for electrophysiological recording as needed for as long as 8 hr after cell isolation. Neurons were viewed using an inverted microscope and GΩ seals were achieved using glass microelectrodes with an impedance of 2–4 MΩ. Whole-cell recordings were performed at room temperature using the EPC-7 (List Electronics, Darmstadt, F.R.G.) patch-clamp amplifier. Neurons were superfused with extracellular medium at 1.5 ml/min. Unless otherwise noted, the "normal" extracellular recording medium contained 150 mM NaCl, 5 mM KCl, 2.5 mM $CaCl_2$, 1 mM $MgCl_2$, 10 mM Hepes, and 10 mM D-glucose; pH was buffered to 7.4 using NaOH and osmolality was adjusted to 340 mmol/kg using sucrose. Unless otherwise noted, the normal solution in the patch pipette (which dialyzed the interior of the neuron) contained 140 mM KCl, 1 mM $CaCl_2$, 2 mM $MgCl_2$, 11 mM EGTA, and 10 mM Hepes; pH was buffered to 7.4 using KOH and osmolality was adjusted to 310 mmol/kg using sucrose. The extracellular solution for Ca^{2+} current isolation consisted of 150 mM tetraethylammonium chloride, 2.5 mM $CaCl_2$, 0.8 mM $MgCl_2$, 10 mM Hepes, and 25 mM D-glucose; pH was buffered to 7.4 with tetraethylammonium hydroxide and osmolality was adjusted to 340 mmol/kg using sucrose. The recording pipet (internal) solution used for Ca^{2+} current isolation contained 140 mM *N*-methyl-D-glucamine, 2 mM tetraethylammonium chloride, 2 mM $MgCl_2$, 10 mM Hepes, and 1.1 mM EGTA; pH was buffered to 7.4 with HCl and osmolality was adjusted to 310 mmol/kg with sucrose.

Neurons included in this study had a diameter between 30 and 50 μm. For experiments in which Ca^{2+} currents were not isolated, neurons were used only if their membrane potential was −40 mV or more negative. Duration of the ADPP was measured from the beginning of the current pulse to the point at which membrane potential had recovered to within 10% of its original value. The time to peak of the ADPP was measured from the beginning of the current pulse. Inactivation curves were fit to a Boltzman function as described by Leibowitz *et al.* (10). Data were sampled and digitized at 2 or 5 kHz by a model 2090-111A Nicolet digital oscilloscope and stored for off-line analysis using a PDP 11/23 microcomputer.

RESULTS

Fig. 1 illustrates burst firing and the effect of membrane potential on this phenomenon. Fig. 1*A* shows voltage recordings from a typical burst-firing neuron whose membrane potential was held at −75 mV. A short depolarizing pulse elicited two spikes that fired at 70 Hz. Both spikes fired on the rising phase of a large depolarizing potential (the ADPP). When the membrane potential of this neuron was depolarized to −66 mV, the depolarizing pulse elicited three spikes that fired at 35–40 Hz upon a reduced-amplitude (ADPP) (Fig. 1*B*). When the membrane potential was further depolarized to −59 mV, the stimulus evoked only a single spike that was followed by an afterhyperpolarization (Fig. 1*C*). The graph in Fig. 1*D* plots the amplitude of the ADPP as a function of

The publication costs of this article were defrayed in part by page charge payment. This article must therefore be hereby marked "*advertisement*" in accordance with 18 U.S.C. §1734 solely to indicate this fact.

Abbreviations: ADPP, afterdepolarizing potential; DRG, dorsal root ganglion.

*To whom reprint requests should be addressed at: Section of Electrophysiology, National Institute on Alcohol Abuse and Alcoholism, 12501 Washington Avenue, Rockville, MD 20852.

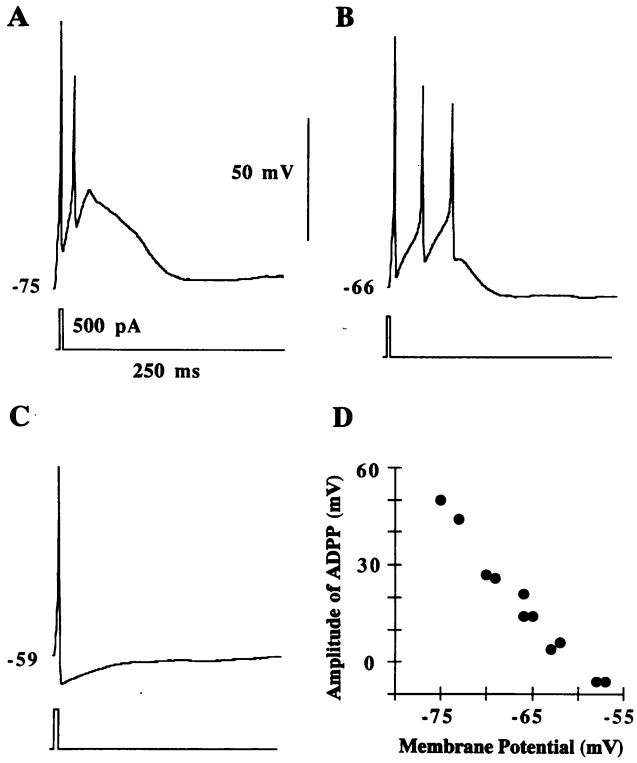

FIG. 1. Effect of membrane potential on burst firing and amplitude of the ADPP. (*A–C*) Upper records are current-clamp recordings of voltage responses; membrane potential was adjusted by constant current injection, as indicated. Lower records indicate a depolarizing current pulse 5 ms in duration and 500 pA in amplitude that evoked the response. (*A*) Burst firing and ADPP elicited from a membrane potential of −75 mV. The current pulse evoked a pair of action potentials that fired on the rising phase of an ADPP. The ADPP peaked in ≈39 ms and had a duration of ≈100 ms. (*B*) Burst firing and ADPP elicited from a membrane potential of −66 mV. The current pulse elicited a burst of three spikes that rode upon a reduced amplitude ADPP. (*C*) Voltage response elicited from a membrane potential of −59 mV. A single spike was elicited by the depolarizing pulse; the spike repolarized rapidly and was followed by an afterhyperpolarizing potential. Neither an ADPP nor burst firing was observed when membrane potential was depolarized positive to −60 mV. (*D*) Graph of ADPP amplitude plotted as a function of membrane potential. From a different neuron than that used in *A–C*.

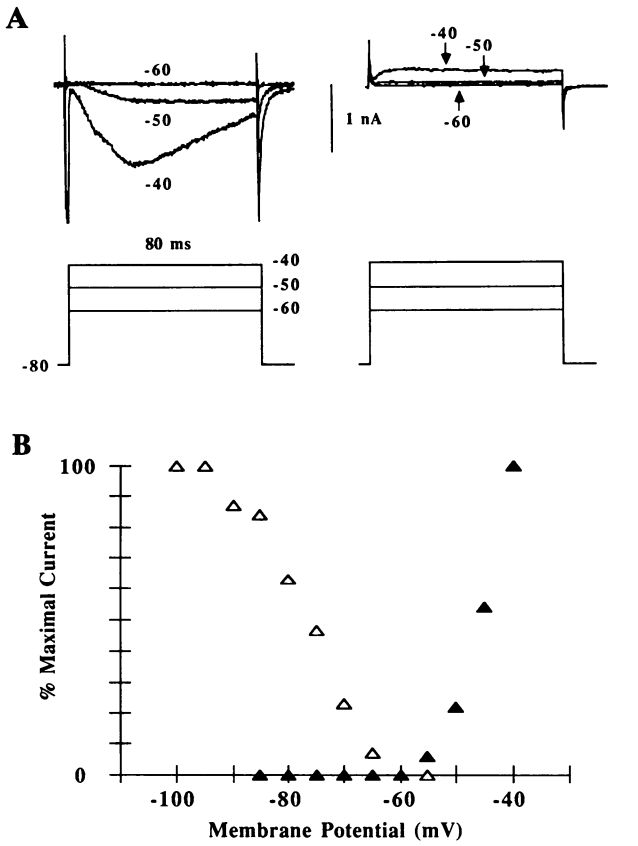

FIG. 2. Voltage-activated current responses. (*A Left*) Current responses in a burst-firing neuron. Voltage-clamp records of currents (upper records) elicited by voltage steps (lower records) to −60, −50, and −40 mV from a holding potential of −80 mV. Note that the inward current activated by the step to −40 mV reached peak amplitude in ≈50 ms and decayed considerably during the 80-ms step. The relatively slow onset of the inward current in this experiment is due to activation near threshold and the lack of a prepulse to achieve maximal activation (e.g., see ref. 11); for comparison with a prepulse, see Fig. 4. (*A Right*) Current responses in a non-burst-firing neuron. Current and voltage records are displayed as in *A Left*. Note that steps to −50 and −40 mV activated only small outward currents; no net inward current was observed at these voltage steps in non-burst-firing neurons. (*B*) Graph-plotting activation and inactivation of the inward current in a burst-firing neuron. ▲, Activation of inward current. Amplitude of inward current (% maximal current) plotted as a function of step potential; holding potential was −80 mV. Note that inward current activated at potentials positive to −60 mV. △, Inactivation of inward current. Amplitude of inward current (% maximal current) plotted as a function of the holding potential. Current was activated by step to −45 mV. Note that the inward current begins to inactivate at holding potentials positive to −95 mV and is completely inactivated at −60 mV.

membrane potential. The amplitude of the ADPP increased progressively as the membrane potential was hyperpolarized below −60 mV. In all cells tested (n = 32), burst firing was observed only in conjunction with an ADPP (n = 19). In neurons that did not exhibit an ADPP at membrane potentials negative to −60 mV (n = 13), the response to a stimulus was similar to the record of Fig. 1*C*.

Since not all neurons exhibited burst-firing behavior, we first attempted to identify the current that underlies this response by looking for a current that was specific to neurons that manifest burst firing. Fig. 2*A* shows records of currents that were evoked in burst-firing (Fig. 2*A Left*) and non-burst-firing (Fig. 2*A Right*) neurons. In each cell type, neuronal membrane potential was stepped from a holding potential of −80 mV to −60, −50, and −40 mV. In the neuron that exhibited an ADPP with burst firing (Fig. 2*A Left*), inward current was first observed with the step to −50 mV. With the step to −40 mV, the current reached peak amplitude in about 50 ms and decayed considerably over the time course of the 80-ms voltage step. Fig. 2*A Right* illustrates a similar series of voltage steps for a neuron in which neither an ADPP nor burst firing was observed. The voltage steps to −50 and −40 mV elicited only small net outward current. A transient low-threshold inward current was not observed in neurons in which an ADPP was not observed (n = 12); whereas this inward current was always present in neurons that had an ADPP (n = 15). In Fig. 2*B*, the amplitude of the inward current is plotted as a function of step potential. The graph shows that the inward current first activated at potentials just positive to −60 mV, indicating a low threshold for activation.

If this transient low-threshold inward current underlies the generation of the ADPP, then the amplitude of both the inward current and the ADPP should be affected in a similar manner by membrane holding potential and ionic manipulations of external and/or internal solutions. To study the effect of membrane holding potential on the inward current, we voltage-clamped the burst-firing type of neurons to holding potentials from −100 to −55 mV in 5-mV increments. From each holding potential, the membrane potential was stepped

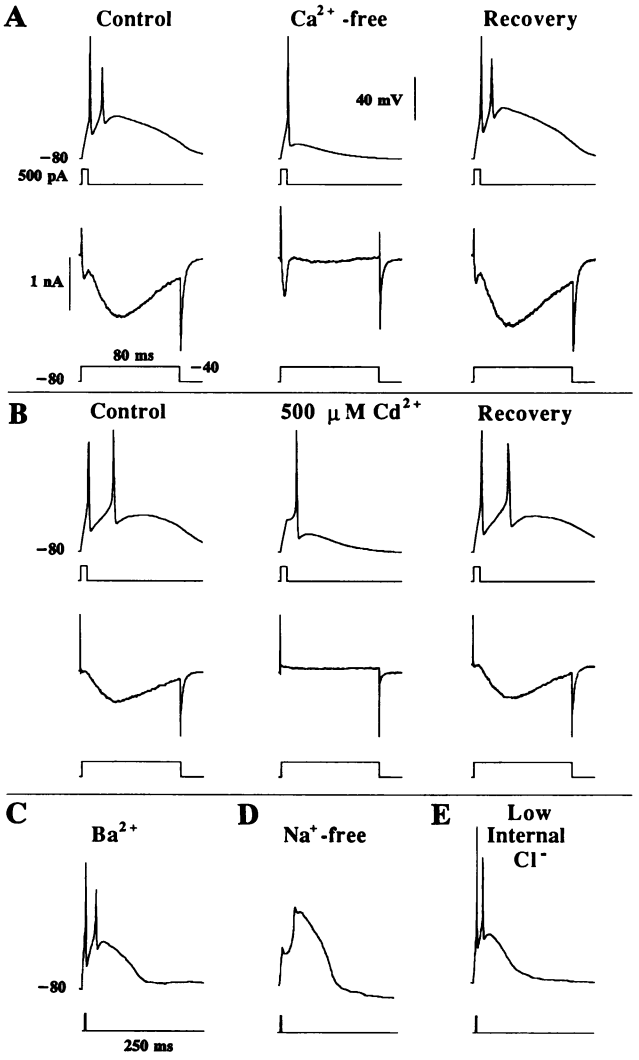

FIG. 3. Effect of ion substitution on voltage (upper records) and current (lower records) responses in burst-firing neurons. (*A*) Effect of substitution of Mg^{2+} for Ca^{2+} in external solution. (*Left*) Control responses with ADPP, burst firing, and transient inward current in a normal (2.5 mM) external Ca^{2+} solution. (*Center*) Responses ≈60 s after beginning superfusion with a solution in which Mg^{2+} was substituted for Ca^{2+}. Note that burst firing ceased, and the amplitude of the ADPP and the inward current were both decreased by >90%. (*Right*) Responses ≈60 s after beginning superfusion with a normal Ca^{2+}-containing solution. Note that burst firing returned, as did the ADPP and the inward current. (*B*) Effect of 500 μM Cd^{2+} in the external solution. (*Left*) Control responses showing ADPP with burst firing and inward current. (*Center*) Responses ≈60 s after beginning application of external solution containing 500 μM Cd^{2+}. Note that burst firing ceased, and the amplitude of the ADPP and the inward current decreased by >90%. (*Right*) Responses ≈60 s after terminating application of Cd^{2+}. Note that burst firing, the ADPP, and the inward current all returned. (*C*) Responses recorded with Ba^{2+} substitution for Ca^{2+} on an equimolar basis in the external solution. (*D*) Responses recorded in a Na^+-free external solution. Na^+ was replaced by $Tris^+$. (*E*) Responses recorded with a low (6 mM) internal Cl^-. The low Cl^- patch pipet solution contained 140 mM $KMeSO_4$, 1 mM $CaCl_2$, 2 mM $MgCl_2$, 3 mM KCl, 11 mM EGTA, and 10 mM Hepes. The ADPP shown in *C–E* and the respective inward currents (data not shown) had characteristics similar to those observed in the presence of the standard solutions described in Fig. 1; namely, time course, threshold of activation, and voltage-dependence of inactivation, indicating that the ionic manipulations in *C–E* did not appreciably influence either the inward current or the ADPP. In addition, burst firing was observed with Ba^{2+} substitution for Ca^{2+} and low internal Cl^-. Burst firing was not observed, however, in Na^+-free external solution, since action potential generation was Na^+-sensitive. Voltage responses were elicited from a holding potential of −80 mV, as in Fig. 1. Currents were elicted from a holding potential of −80 mV by stepping to −45 mV for 80 ms. Ion substitutions were applied by lowering a macropipet (20–40 μm, tip diameter) to within 30 μm of the neuron. Ion substitution was terminated by withdrawing the macropipet. The records in *A–E* are from different neurons. The voltage (mV) and current calibrations in *A* apply to all records. Time scales in *A* apply to *B*; the time scale in *C* applies to *D* and *E*. Note that the time scales are the same for voltage and current traces in *A* and *B*.

to −45 mV. In Fig. 2*B*, the amplitude of the inward current elicited in this manner is plotted as a function of holding potential. The graph illustrates that the inward current was first observed when the holding potential was negative to −60 mV and increased in amplitude at more negative holding potentials to a maximum near −95 mV. This effect of a membrane holding potential is similar to that observed for the ADPP (compare to Fig. 1*D*).

To determine if the ionic sensitivities of the ADPP and the inward current are similar, we first tested whether extracellular Ca^{2+} is necessary for generation of both the inward current and the ADPP. Neurons were superfused with a Ca^{2+}-free solution in which external Ca^{2+} was replaced by Mg^{2+}, which is a relatively impermeant divalent cation (12). Under these conditions, both the inward current and the ADPP decreased by >90% and burst firing was eliminated (Fig. 3*A*). To test further whether the inward current and the ADPP were dependent upon flux through Ca^{2+} channels, neurons were superfused with 500 μM Cd^{2+}, a Ca^{2+} channel blocker (12). In the presence of Cd^{2+}, the amplitude of both the inward current and the ADPP decreased by >90% and burst firing was eliminated (Fig. 3*B*). These observations suggest that the inward current and the ADPP require Ca^{2+} influx. The possibility that the ADPP might be generated by a Ca^{2+}-activated current (13–16) was tested by substitution of Ba^{2+} for Ca^{2+} in the external solution [Ba^{2+} can carry current through Ca^{2+} channels (12) but does not elicit Ca^{2+}-activated currents in most neurons (15–17)]. Fig. 3*C* shows that after substitution of equimolar Ba^{2+} for Ca^{2+} in the external bath, the ADPP with burst firing was still observed. If the ADPP is generated by a Na^+ current, then the ADPP should not be observed in the absence of extracellular Na^+. As can be seen in Fig. 3*D*, a Na^+-free superfusate abolished the Na^+-dependent action potentials but the ADPP was still present. The contribution of Cl^- to the generation of burst firing and the ADPP was tested using a low Cl^- (6 mM) internal solution. With this internal solution, an increase in Cl^- conductance would generate a membrane hyperpolarization. Fig. 3*E* shows that the ADPP with burst firing was present with this low internal Cl^- solution. These observations suggest that the ADPP is generated by a Ca^{2+} current rather than a Ca^{2+}-activated current.

Since the ADPP appears to result from activation of a Ca^{2+} current, the inward current was studied further in solutions designed to isolate Ca^{2+} currents. Fig. 4*A* illustrates the inward current elicited from a holding potential of −100 mV by a step to −45 mV in solutions designed to isolate Ca^{2+} currents. The transient nature of the current is evident in that it reaches peak amplitude in ≈12 ms and decays considerably over the course of the 80-ms pulse. Currents of smaller amplitude were evoked by stepping to −45 mV from potentials depolarized to −100 mV (Fig. 4*B*). Fig. 4*B* also shows that the inward current first activated when stepping to −65 mV from −80 mV and attained maximal amplitude near −35 mV. The time-course, activation and inactivation properties of this current are similar to the properties of the inward current associated with ADPP generation in normal solutions and a transient low-threshold (T-type) Ca^{2+} current described in cultured DRG neurons and other cell types (11, 18–20). For example, after fitting inactivation data points to a Boltzman

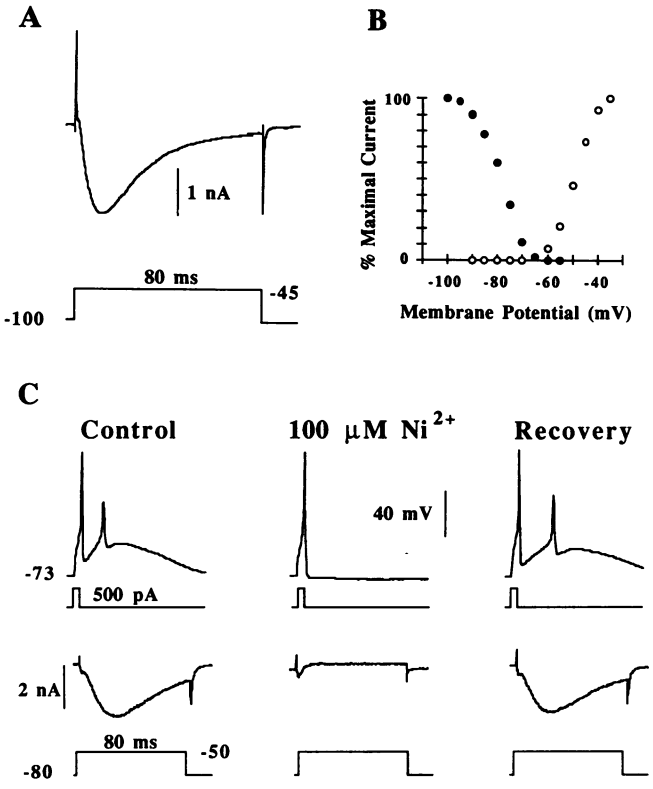

FIG. 4. Properties of the low-threshold inward current. (*A*) Record of the current elicited by a voltage step to −45 mV from a holding potential of −100 mV in solutions designed to isolate Ca^{2+} currents. Note that the current reaches peak amplitude ≈12 ms after the onset of the voltage step and decays considerably during the 80-ms step. (*B*) Graph of activation and inactivation characteristics from neuron illustrated in *A*. ○, Activation of inward current in Ca^{2+} current isolation solutions. Amplitude of inward current (% maximal current) plotted as a function of step potential; holding potential was −80 mV. Note that threshold for current activation was −65 mV. ●, Inactivation of inward current in Ca^{2+} current isolation solutions. Amplitude of inward current (% maximal current) plotted as a function of holding potential. Current was activated by step to −45 mV. Note that inward current begins to inactivate at holding potentials positive to −100 mV and is completely inactivated at −60 mV. Also note the similarity between the activation and inactivation characteristics of the inward current in normal solutions compared to solutions designed to isolate Ca^{2+} currents (compare Figs. 2*B* and 4*B*). (*C*) Effect of Ni^{2+} on ADPP with associated burst firing and the inward current in normal external and internal solutions. (*Left*) Control responses showing ADPP with burst firing and inward current. (*Center*) Responses ≈60 s after beginning application of external solution containing 100 μM Ni^{2+}. Note that burst firing ceased and both the ADPP and the inward current were no longer detectable. (*Right*) Responses ≈60 s after terminating application of Ni^{2+}. Note that burst firing, the ADPP, and the inward current all returned to control conditions. All responses are from the same neuron in current- (*Upper*) and voltage- (*Lower*) clamp conditions. Time scale is the same for both current and voltage pulses. Other conditions are as in Fig. 3.

function, the membrane potential at which half-inactivation of the current occurred was −82 ± 2 mV (n = 6), which is similar to values reported for the T-type Ca^{2+} current by others (for example, see ref. 20). In addition, the transient low-threshold inward current observed in solutions designed to isolate Ca^{2+} currents was eliminated by 100 μM Ni^{2+}, while higher threshold Ca^{2+} current was much less affected. This sensitivity of voltage-activated Ca^{2+} current to Ni^{2+} is similar to that reported for the T-type Ca^{2+} current (20). We, therefore, tested the effects of Ni^{2+} on both the ADPP and its associated burst firing as well as on the presumed T-type Ca^{2+} current in normal internal and external solutions. As illustrated in Fig. 4*C*, the ADPP and its associated burst firing was completely eliminated in the presence of Ni^{2+} (100 μM), as was the transient inward Ca^{2+} current. On the other hand, the dihydropyridine, nifedipine (10 μM), had no effect on the ADPP and its associated burst firing or on the amplitude of the transient inward current (data not shown).

DISCUSSION

The observations presented in this report indicate that a transient low-threshold (T-type) Ca^{2+} current underlies the generation of the ADPP that triggers burst firing in a subpopulation of DRG neurons. ADPPs with properties similar to those described here have also been observed in neurons in the central nervous system. For example, in entorhinal cortex, an area associated with information processing and seizure development, an ADPP that elicits burst firing is observed only in neurons that have been hyperpolarized negative to −60 mV (21). In neurons of the visual cortex (22) and most thalamic nuclei (3, 23, 24), ADPPs that elicit burst firing have been reported to have a voltage and/or Ca^{2+} dependence similar to that described here. It has also been suggested that a low-threshold, voltage- and Ca^{2+}-sensitive ADPP may be important in the generation of oscillatory behavior in neurons of the inferior olive (7, 25, 26) and other brain regions (7, 27–29). The similarity of the properties of the ADPP that triggers burst firing in central and DRG neurons suggests that a transient low-threshold Ca^{2+} current may generate burst firing in several areas of the mammalian nervous system.

The properties of the transient low-threshold Ca^{2+} current suggest that burst firing may be modulated in at least two ways. (*i*) The voltage sensitivity of the current indicates that the membrane potential of the neuron will affect the amplitude of the current and consequently the burst-firing pattern. Thus, factors that affect membrane potential, such as neurotransmitters, neurohormones, or the concentration of extracellular K^+, would be expected to affect burst-firing behavior. (*ii*) Burst firing may also be modulated by other factors that change the amplitude of the transient low-threshold Ca^{2+} current. For example, we have found (30) that the neurotransmitter glutamate inhibits the T-type Ca^{2+} current in DRG neurons and thereby alters burst firing in these neurons. Further work will no doubt reveal other factors that can affect T-current amplitude and thereby regulate burst-firing behavior (31, 32). Since the burst-firing phenomenon is involved in the processing of neural information, the observation that the T current underlies burst-firing behavior and the fact that the T current can be regulated by various physiologic factors suggest that the T current may play an important role in the regulation of information processing in the nervous system.

1. Kandel, E. R. & Spencer, W. A. (1961) *J. Neurophysiol.* **24**, 243–259.
2. Llinas, R. & Sugimori, M. (1980) *J. Physiol. (London)* **305**, 147–213.
3. Jahnsen, H. & Llinas, R. (1984) *J. Physiol. (London)* **349**, 205–226.
4. Sumitomo, I., Takahashi, Y., Kayama, Y. & Ogawa, T. (1988) *Brain Res.* **447**, 376–379.
5. Eccles, J. C. (1983) *Neuroscience* **10**, 1071–1081.
6. Thompson, R. F. (1986) *Science* **233**, 941–947.
7. Llinas, R. R. (1988) *Science* **242**, 1654–1664.
8. McNamara, J. O., Byrne, M. C., Dasheiff, R. M. & Fitz, J. G. (1980) *Prog. Neurobiol.* **15**, 139–159.
9. Racine, R. (1978) *Neurosurgery* **3**, 234–252.
10. Leibowitz, M. D., Sutro, J. B. & Hille, B. (1986) *J. Gen. Physiol.* **87**, 25–46.
11. Bossu, J.-L. & Feltz, A. (1986) *J. Physiol. (London)* **376**, 341–357.

12. Hagiwara, S. & Byerly, L. (1981) *Annu. Rev. Neurosci.* **4,** 69–125.
13. Suarez-Kurtz, G. (1979) *J. Physiol. (London)* **286,** 317–329.
14. Owen, D. G., Segal, M. & Barker, J. L. (1986) *J. Neurophysiol.* **55,** 1115–1135.
15. Mayer, M. L. (1985) *J. Physiol. (London)* **364,** 217–239.
16. Korn, S. J. & Weight, F. F. (1987) *J. Neurophysiol.* **58,** 1431–1451.
17. Gorman, A. L. F. & Hermann, A. (1979) *J. Physiol. (London)* **296,** 393–410.
18. Carbone, E. & Lux, H. D. (1984) *Nature (London)* **310,** 501–502.
19. Nowycky, M. C., Fox, A. P. & Tsien, R. W. (1985) *Nature (London)* **316,** 440–443.
20. Fox, A. P., Nowycky, M. C. & Tsien, R. W. (1987) *J. Physiol. (London)* **394,** 173–200.
21. Jones, R. S. G. & Heinemann, U. (1988) *J. Neurophysiol.* **59,** 1476–1496.
22. Artola, A. & Singer, W. (1987) *Nature (London)* **330,** 649–652.
23. Deschenes, M., Paradis, M., Roy, J. P. & Steriade, M. (1984) *J. Neurophysiol.* **51,** 1196–1219.
24. Jahnsen, H. & Llinas, R. (1984) *J. Physiol. (London)* **349,** 227–247.
25. Llinas, R. & Yarom, Y. (1981) *J. Physiol. (London)* **315,** 569–584.
26. Llinas, R. & Yarom, Y. (1986) *J. Physiol. (London)* **376,** 163–182.
27. Burlhis, T. M. & Aghajanian, G. K. (1987) *Synapse* **1,** 582–588.
28. Nakanishi, H., Kita, H. & Kitai, S. T. (1987) *Brain Res.* **437,** 35–44.
29. Murase, K. & Randic, M. (1983) *J. Physiol. (London)* **334,** 141–153.
30. Lovinger, D. M. & Weight, F. F. (1988) *Soc. Neurosci. Abstr.* **14,** 792.
31. Twombly, D. A., Yoshii, M. & Narahashi, T. (1988) *J. Pharmacol. Exp. Ther.* **246,** 189–195.
32. Coulter, D. A., Huguenard, J. R. & Prince, D. A. (1988) *Soc. Neurosci. Abstr.* **14,** 644.